Phenomenology of Hadronic Interactions at Intermediate Energies

M. Fukugita

Department of Physics, University of Tokyo
Tokyo, Japan

A note on the talk at the Summer School held at National Laboratory for High Energy Physics (Japan) on 17 - 21 July, 1972.

1. Introduction

It is well known that high energy scattering shows fairly smooth energy dependence and can be described qualitatively in terms of the crossed channel Regge exchange. There are a lot of analyses of high energy scattering above $p_{Lab} = 3 \sim 5$ GeV/c along this line.[1] Recent experiments, however, suggest that the properties of Regge exchange persist even in the intermediate (or low) energy region such as $p_{Lab} = 1 \sim 3$ GeV/c.

For example, the polarization in $\pi^{\pm}p$ scattering at $p_{Lab} = 1.6 \sim 2.3$ GeV/c[2] shows a remarkable similarity to the polarization at higher momentum which is attributed to the interference between the ρ and P + P Regge exchanges. Furthermore, the low energy extrapolation of the phenomenological Regge fit[3] can reproduce this polarization fairly well (fig.1). Similarly the polarization in K^+p[4] and K^-p[5] scattering at p_{Lab} 2 GeV/c has a strong resemblance to that expected from the interference between the $\rho + A_2$ and $P + P'$ Regge exchanges. Besides these examples, there are many cases which indicate the validity of the Regge exchange picture in such low energy region.

At low and intermediate energies, from threshold to p_{Lab} 2 GeV/c, inelastic scattering such as charge exchange reaction is dominated by direct-channel resonances (e.g. fig.2). [Elastic scattering, of course, contains the large nonresonant background contribution from diffraction scattering]. Although this description by resonances appears very different from the description by Regge exchanges, two descriptions are related

through the analyticity of scattering amplitudes*. Actually, the contribution of resonances (and possible background) on the average over low energies are already contained in the Regge exchanges.[6] In terms of the finite energy sum rules,[7] the sum of low energy amplitude builds the Regge exchange. Furthermore, it is believed that the sum of resonances builds the ordinary Regge exchange and the sum of the background the pomeron Regge exchange.[8]

The validity of the Regge exchange picture in the resonance region, however, implies the existence of more direct relations between resonances and Regge exchange. In this energy region up to 2 GeV/c many partial wave analyses have been performed to determine the resonance parameters. Partial wave solutions enable us to determine the scattering amplitudes in the resonance region and to investigate to what extent the duality actualy holds.[9]

In this note we mainly focus our attention on the resonant part of the amplitude which is considered to build the ordinary Regge exchange. We present the results of the analyses by making use of partial wave data, and discuss their implications to the model of hadronic reactions at higher energy.

---

* The relation between direct-channel (s-channel) description and crossed channel (t-, or u-channel) description is called duality.

2. Analysis of $K^{\pm}N$ scattering[9]

We begin with the analysis of kaon-nucleon scattering. In terms of Veneziano model,[10] the gross features of kaon-nucleon scattering amplitude are expressed as

$$\frac{\Gamma(1-\bar{\alpha}(s))\Gamma(1-\alpha(t))}{\Gamma(1-\bar{\alpha}(s)-\alpha(t))},$$

apart from the background part. Where $\bar{\alpha}(s)$ and $\alpha(t)$ are $Y^{*}_{0,1}$ and ρ-A_2, f-ω trajectories, respectively. The simplicity of this expression suggests us that $K^{\pm}N$ scattering may be the most appropriate case to test the duality.

We now summarize briefly the procedure of the analysis. In order to study the relation between the s-channel description and t-channel Regge exchange picture, we work with the t-channel isospin combinations of the s-channel helicity amplitudes without the kinematical factors,

$$\bar{f}_{++} \equiv f_{++}/\cos\frac{\theta}{2} = f_1 + f_2, \quad \bar{f}_{+-} = f_{+-}/\sin\frac{\theta}{2} = f_1 - f_2.$$

We mainly study the behaviour of the imaginary parts of these amplitudes, reconstructing the resonant and background amplitudes separately from partial wave solutions, in which partial waves are given by the sum of resonances and background contributions. As the imaginary parts of the non-diffractive scattering amplitudes are expected to be dominated locally by the nearby resonances, the imaginary parts are more appropriate for our aim to test the

duality. Before making the analysis, we have selected partial wave solutions obtained by several groups, by comparing them with new accurate data as far as possible. In table 1, we exhibit the partial wave solutions which are used in the following analysis.

Test of the Harari-Freund conjecture

Before arguing the nature of the resonant part, we briefly mention the properties of the background part, in order to test the Harari-Freund conjecture which permits us to treat the resonant and background parts separately.

In fig.3, we present the t-dependence of $qImf_{++}^{B.G.}$ and $qImf_{+-}^{B.G.}$ constructed from the background parts of $\bar{K}N$ partial wave solutions. The $I_t = 0$ and $I_t = 1$ amplitudes show a remarkable contrast; the $I_t = 0$ helicity nonflip amplitude has a large forward peak and exhibits a diffraction-like t-dependence, whereas the $I_t = 1$ amplitudes are considerably smaller in the small t-region. The t-dependences of $qIm\bar{f}_{++}$ constructed from the K^+p and K^+n partial waves are shown in fig.4. We can see that the properties of KN amplitudes are very similar to those of $\bar{K}N$ background amplitudes.

To make quantitative studies, we present in fig.5 the forward amplitude of $qImf_{++}^{B.G.}$, $I_t = 0$ calculated from the background part of $\bar{K}N$ partial waves. This value corresponds to $\sigma_{tot} \simeq 20$ (mb) which is considered to be the total cross section at high energy, i.e., approximately the cross section of pomeron exchange. In addition to this the slope of the background amplitude shows the shrinkage as is seen in K^+p, pp and ϕp scattering.[18]

These results are in excellent agreement with the conjecture[8] that the background part builds the pomeron exchange.

Imaginary part of the resonant amplitude

The t-dependence of the imaginary parts of the resonant amplitudes at various incident momenta are shown in fig.6. The following features can be read from the figures.

(i) $q\mathrm{Im}\bar{f}^{\mathrm{res.}}_{++}$, $I_t = 0$ and $q\mathrm{Im}\bar{f}^{\mathrm{res.}}_{+-}$, $I_t = 1$ show a fairly energy independent pattern in the small $|t|$ region: their signs are definite at $t = 0$ and in accord with those expected from the crossed channel pole exchange; They pass through a zero at approximately fixed t, i.e., at $t \simeq -0.2$ and -0.45 $(\mathrm{GeV/c})^2$, respectively. These features are interpreted as demonstrating that the t-channel Regge exchange picture persists even at $p_L = 1 \sim 2$ GeV/c, though the total cross section has large fluctuation in s in this energy region. In Regge pole language, the zero at $t \simeq -0.5$ $(\mathrm{GeV/c})^2$ is usually attributed to the passing of the ρ-A_2 trajectory through a nonsense point ($\alpha_\rho(t) = 0$). The other zero at $t \simeq -0.2$ is introduced empirically in the Regge residue function, in order to explain the crossover effect, in conventional Regge pole models.*

---

* From the viewpoint of Regge-cut models, this crossover zero is also interpreted as the nonsense zero which is moved to the forward direction by the absorptive correction.

(ii) For $I_t = 0$, $q\mathrm{Im}\bar{f}^{res}_{+-}$ and $q\mathrm{Im}\bar{f}^{res}_{++}$ change their shapes when p_{Lab} is varied; zeros are missing at some values of p_{Lab} and even the signs of the amplitudes at $t = 0$ are not definite. Further, these amplitudes are much smaller than the other two, when they are averaged over a momentum interval.

Previously, Dolen, Horn and Schmid[19] have pointed out that we can affirm that the first zero of Legendre polynomials in the resonance summation occurs at a fixed t if we assume a tower of direct channel resonances with spin ℓ_R and momentum q_R which satisfy the relation $\ell_R \approx R \cdot q_R$. In the case of $\bar{K}N$ scattering, at least in the energy region of this analysis, two series of leading resonances, Λ_α-Λ_γ and Σ_δ-Σ_β, which lie on the line $R \approx 1$ fm,[20] dominate the imaginary part of the amplitudes (See fig.7). The series Λ_α-Λ_γ and Σ_δ-Σ_β add for $\mathrm{Im}\bar{f}_{++}$, $I_t = 0$ and $\mathrm{Im}\bar{f}_{+-}$, $I_t = 1$, hence these amplitudes exhibit the fixed t zeros at $t \sim -0.2$ and ~ -0.45, respectively, as the first zeros of the d-functions $d^J_{1/2\ 1/2}(\cos\theta) \simeq P_\ell(\cos\theta) \approx J_0(R\sqrt{-t})$ (helicity nonflip) and $d^J_{-1/2\ 1/2} \simeq P'_\ell(\cos\theta) \approx J_1(R\sqrt{-t})$ (helicity flip).

On the other hand, a large cancellation occurs between the contributions of the two series, Λ_α-Λ_γ and Σ_δ-Σ_β, to $\mathrm{Im}\bar{f}_{+-}$, $I_t = 0$ and $\mathrm{Im}\bar{f}_{++}$, $I_t = 1$. As a consequence these amplitudes are quite small and the zeros of these amplitudes vary irregularly as the energy changes. Then they do not exhibit regularities expected from Regge exchange in the low energy region such as $p_{Lab} = 1 \sim 2$GeV/c.

This correlation among the direct channel resonances accounts for the helicity conservation of the f-ω Regge exchange and helicity flip character of the ρ-A_2 Regge exchange.

Real part of the resonant amplitude

We now briefly mention the real part of the resonant amplitude. Since the real part is not controlled locally by the nearby resonances, we cannot separate the full amplitude into background and resonant parts as in the case of the imaginary part. Then we take the inelastic scattering amplitude which is considered to consist only of resonant amplitude.

We present the t-dependence of the $I_t = 1$ Re $\bar{f}_{+-}$ in fig.8 at several values of p_{Lab}. When averaged in incident momenta, they show the t-dependence as $\sim \cos\pi\alpha(t)$ which is expected from the ρ-A_2 exchange degenerate Regge pole exchange.

In order to make comparison, we show, in fig.9, $\mathrm{Re}[f_{+-}(K^-p) - f_{+-}(K^+p)]$, exhibiting the t-dependence as $\sim -\sin^2 \frac{\pi\alpha(t)}{2}$ when averaged in p_{Lab}. This behaviour is also expected from the vector (ρ and ω) Regge exchange.

3. Correlation of resonances and Regge exchange

In the resonance region such as $p_{Lab} \lesssim 2$ GeV/c, large fluctuations are obviously seen in total cross sections of hadronic reactions, as the energy varies. However, as we have seen in the preceding section, the imaginary parts of the amplitudes, which consist essentially of the sum of the contributions of a few nearby resonances,* already show, particularly in their t-dependences, the properties of Regge exchanges, if we take the amplitudes in which the prominent resonances correlate constructively with each other. When energy increases and the widths of resonances become larger as compared with their intervals, we expect that the sums of resonances at that energies will show the smooth energy dependence, while the t-dependence still remains unchanged if we assume the towers of resonances with $\ell_R \approx R \cdot q_R$. [In reality, as implied by the original Veneziano model,[10] there may exist** resonances near the energy $\sqrt{s}$, with spins from $J_R = 1/2, (3/2), 5/2, \cdots$, probably to $J_R = \alpha(s)$, while the coupling strengths of these resonances take their maximum at $J_R \approx R \cdot q_R$. Hence the resonances

---

* For the real parts, since the contribution from the tails of far-off resonances is important, we cannot make a simple discussion.

** A single or several towers of resonances are insufficient to satisfy the finite energy sum rule.[35]

with large coupling strengths may form a peripheral band* along $J \approx R \cdot q$ (i.e. impact parameter $b \approx R$).] From this viewpoint, we can easily understand the conjecture[23] that the partial wave expansion of the Regge amplitude makes resonances.

On the other hand, the imaginary parts of the amplitudes in which a large cancellation between resonances occurs exhibits large fluctuations in the low energy regions. As the widths of resonances grow sufficiently large, the amplitude will show Regge-like t-dependence and the smooth energy dependence, though the magnitude of the amplitude will be quite small.

We have assumed, in this argument, the existence of resonances at high energies such as $p_{Lab} = 5$ GeV/c. At present, resonances are established only up to $p_{Lab} = 2.5$ GeV/c or so. As energy increases, the resonance becomes more collective,** the widths of individual resonances become larger, and what is worse they become more inelastic. Therefore the search for resonances becomes exceedingly difficult. In addition to this, the rise of many high partial waves makes it almost impossible to perform

---

*, ** To assure the Regge behaviour $s^{\alpha(t)}$, the width of peripheral band Δb must increase as $\Delta b \sim (\log s)^{1/2}$ with increasing energy. We should not confuse <u>the width of the peripheral band</u> with the <u>width of individual resonances</u>. The former has little to do with the latter.

partial wave analyses by usual method. The method to treat several partial waves collectively, i.e., the phase hand method[24] might provide the way to search resonances, at least to give the partial wave profiles at such energies. Investigations in this direction, anyhow, are very important to understand hadron dynamics.

We present, in the next section, examples of the results to support the above mentioned picture.

4. Further examples exhibiting the aspects of duality

Local duality of πN scattering[21]

We make the partial wave projection of phenomenological Regge fit[3] for $\pi^- p \to \pi^0 n$ reaction after Schmid,[23] and compare the partial wave profile with that calculated from the partial wave solution by Almehed and Lovelace.[25] The fig.10 shows these two profiles of q $\mathrm{Im} f^J_{+-}$ ($f^J_{+-} = f_{\ell+} - f_{(\ell+1)-}$ with $\ell = J - 1/2$) at two different energies. The former profiles which are drawn by the ρ Regge exchange have the peripheral peaks, but they are not in agreement with the latter which includes the contribution from backward baryon exchanges as well as the ρ exchange. As is easily understood, the partial waves of the backward baryon exchanges, where N_α is dominant, will contribute constructively to the combination of direct channel resonances $\Delta_\delta + N_\gamma$, and destructively to the combination of $N_\alpha - N_\beta$. Hence the partial waves of the ρ exchange will be smaller than actual partial waves in magnitude at J = 3/2, 7/2, •••• and larger at J = 5/2 9/2, •••. The features seen in the figure are qualitatively in good agreement with the above expectations except for J = 1/2.*

---

* We need information over the whole angles, when we make a partial wave decomposition for low partial waves, particularly for J = 1/2. Therefore the partial wave J = 1/2 (possibly J = 3/2, •••) should not be taken too seriously.

Properties of Regge couplings

The helicity properties of Regge couplings to $N\bar{N}$ are determined by the correlations of direct channel resonances. At the end of Sect.3, we have considered the case of $\bar{K}N$ scattering. In table 2, we summarize the prominent series of resonances in several processes and their correlation in each amplitude.

The properties of Regge couplings obtained by this observation show qualitative agreement with the results which are obtained from the photon coupling under the assumption of vector dominance, as well as the results of phenomenological Regge fits.[26]

In this table, $\bar{K}N \to \pi\Lambda$ shows somewhat different situation, i.e., the contributions of Σ_α and Σ_δ have trends to cancel those of Σ_γ and Σ_β respectively* in both helicity amplitudes. Indeed, the magnitude of Σ_α is roughly equal to Σ_γ and Σ_δ to Σ_β,[28] and this cancellation (See fig.11) is regarded as the evidence of the anti-exchange degeneracy required by the duality diagrams.[29] Although this cancellation makes the imaginary parts quite small, the real parts owing to the far-off N^* resonances in the u-channel build the forward peak in this channel.

---

* Relative phases among Σ_α, Σ_γ, Σ_δ and Σ_β are determined by the partial wave analyses.[27]

Nucleon exchange[30]

So far we have delt with the case of meson exchange. We now refer to baryon exchange. In the baryon exchange processes, we can easily obtain informations about the crossed channel reactions, while it is difficult in the meson exchange processes.

For example, we take the nucleon exchange (i.e., $I_u = 1/2$) in πN scattering. Applying the method mentioned in Sect.3 to this process,* we have obtained the following results.

(i) The signs of helicity nonflip and flip amplitudes are definite and in agreement with the N_α exchange at $u' = 0$ ($u' = u - u_{max}$) in the energy range from $p_{Lab} = 1.0$ to 2.0 (GeV/c).

(ii) Both amplitudes have a zero at $u' = -0.1 \sim -0.3$ $(GeV/c)^2$ and considered to be the wrong signature nonsense zero ($\alpha(u) = -1/2$) of the N_α Regge exchange.

When the amplitude which consists of direct channel resonances, essentially N_α, N_β, N_γ and Δ_δ, is extrapolated to $u = M_N^2$, we may obtain the nucleon Born amplitude of crossed channel scattering. Under the assumption of the nucleon Regge exchange, we have

$$\frac{g_r^2}{4\pi} = -\frac{2}{3\pi}\left[\frac{d\alpha}{du}\right]^{-1} \frac{1}{4\pi} \mathrm{Im}\langle B(s, u = M_N^2)\rangle .$$

---

* We have used the partial wave solution of Almehed and Lovelace,[25] which reproduces recent data of πN backward scattering fairly well.

We present the right hand side of this equation in fig.12 as a function of p_{Lab}. The value obtained is quite consistent with the πNN coupling constant $g_r^2/4\pi = 14.6$.

The exchange degeneracy in $\bar{K}N$ scattering

The coupling strengths of Λ_α and Σ_δ are approximately equal to those of Λ_γ and Σ_β, respectively, owing to the exoticity of KN channels.[31] Since direct channel resonances $\Lambda_\alpha(\Sigma_\delta)$ make the backward peak in the positiue sign, while $\Lambda_\gamma(\Sigma_\beta)$ do it in the negative sign (fig.13),[32] large cancellation occures in the backward amplitude of $\bar{K}N$ scattering as the widths of the resonances increase. Therefore the backward peak of $\bar{K}N$ scattering falls off rapidly with increasing energy,[33] in contrast to the nonexotic cases, say, πN backward scattering.

5. Difficulties of Regge exchange description

In the previous sections, we have observed the qualitative features of scattering amplitudes in terms of the s-channel resonance description. Although we have often refer to Regge exchange, we have so far set aside the problem of zero-systematics of Regge amplitude. In the resonance picture, the position of the first zero of the imaginary part of the scattering amplitude is given by the first zero of the resonances dominant at that energy. Namely the zeros of helicity nonflip and flip amplitudes are given by the first zeros of $P_\ell(\cos\theta)$ and $P_\ell'(\cos\theta)$, respectively. As the partial wave profile of the helicity nonflip amplitude is not too different from that of flip amplitude, at least at intermediate energies, the first zero in the nonflip amplitude is usually closer to the forward direction than in the flip amplitude. This means that the spin structure of the direct channel resonances breaks the exchange degeneracy of the t-channel Regge exchange.[34]

On the other hand, in explicit models incorporating exchange degeneracy, e.g., Veneziano model in which the zeros made by the resonances coincide with the nonsense zeros of the Regge pole exchange[35], low partial wave daughter resonances ($\ell << q\cdot R$, with $R \simeq 1$ fm) strongly contributes to the nonflip amplitude, while, in the flip amplitude, the contribution of daughter resonances are appropriately suppressed so that both zeros in flip and nonflip amplitudes occur at the same position. Regge pole amplitude*

---

* We consider the amplitude such as

$$F(s,t) \sim \frac{1}{\Gamma[\alpha(t)]} \frac{\mp 1 - e^{-i\pi\alpha(t)}}{\sin\pi\alpha(t)} \left[\frac{s}{s_0}\right]^{\alpha(t)}$$

with exchange degeneracy, of course, inherits these features.

Several amplitude analyses, however, exhibit the considerable suppression of low partial wave ($\ell \ll q \cdot R$) contribution to the imaginary parts of both helicity amplitudes at high energy too. The imaginary part of helicity nonflip amplitude as well as that of helicity flip amplitude shows distinct peripheral peaks, as seen in fig.14. As for the helicity flip amplitude, the Regge pole model with exchange degeneracy or Veneziano model, gives a good description for both real and imaginary parts of the amplitudes.

It is widely believed that the morbid behaviour of Regge pole amplitude can be remedied by taking account of the Regge cut contribution, although no credible method of calculating Regge cut is yet known. There have been many trials along this line,[37] but all of the calculations so far carried out seem to fail to present the correct behaviour of scattering amplitudes, particularly in their real part and the energy dependence at large angle.

In this note, we have seen that the sum of direct channel resonances has the qualitative features of crossed channel Regge exchange. Therefore, resonances does not mearly play a dominant role in describing the scattering amplitude at low energies, but they also describe the scattering amplitudes even at high energies where no individual resonances are observed experimentally.

The problem of resonance spectra, i.e., how to derive the coupling strengths as well as the masses of the resonances, is very important to understand the dynamics of hadronic interactions.

Acknowledgement

The author would like to thank Professor H. Miyazawa for the reading of the manuscript. He is also greatful to Dr. Y. Oyanagi for his critical reading and invaluable discussions, and acknowledges to Dr. T. Inami, with whom a part of the analysis was completed.

1. for example
P. D. B. Collins, Phys. Repport 1 C (1971)
2. G. Burleson et al. Phys. Rev. Letters 26 (1971) 338
D. Hill et al. Phys. Rev. Letters 27 (1971) 1241
3. V. Barger and R. J. N. Phillips, Phys. Rev. 187 (1969) 2210
4. B. Barnett et al. Phys. Letters 34B (1971) 655
5. S. Andersson-Almehed et al., Nucl. Phys. B21 (1970) 515
6. R. Dolen, D. Horn and C. Schmid, Phys. Rev. Letters 19 (1967) 402
7. Igi and Matsuda Phys. Rev. Letters 18 (1967) 625
8. H. Harari Phys. Rev. Letters 20 (1968) 1395
P. G. O. Freund Phys. Rev. Letters 20 (1968) 235
9. M. Fukugita, T. Inami and Y. Kimura,
Phys. Letters 36B (1971) 575
M. Fukugita and T. Inami, Nucl. Phys. B44 (1972) 490
10. G. Veneziano Nuovo Cim. 57A (1968) 190
11. C. Bricman, M. Ferro-Luzzi and J. P. Lagnaux
Phys. Letters 33B (1970) 511
12. B. Conforto et al. Nucl. Phys. B34 (1971) 41
13. P. J. Litchfield et al., Nucl. Phys. B30 (1971) 125
14. M. G. Albrow et al. Nucl. Phys. B30 (1971) 273
15. G. Giacomelli et al. Nucl. Phys. B20 (1970) 301
16. B. C. Wilson et al. Glasgow preprint (1972)
17. M. Fukugita and T. Inami, unpublished
18. for example
V. Barger and D. Cline, Nucl. Phys. B23 (1970) 227

19. R. Dolen, D. Horn and C. Schmid
Phys. Rev. 166 (1968) 1768

20. M. Imachi, S. Otsuki and F. Toyoda
Prog. Theor. Phys. 43 (1970) 1105

21. M. Fukugita and T. Inami
Rutherford High Energy Lab. preprint (1972) RPP/T/32

22. for example,
R. Odorico, S. Garcia and C. A. Garcia-Canal
Phys. Letters 32B (1970) 375

23. C. Schmid Phys. Rev. Letters 20 (1968) 689

24. D. Bridges, M. J. Moravcsik and A. Yokosawa
Phys. Rev. Letters 25 (1970) 770
and 26 (1971) 155 (E)

25. S. Almehed and C. Lovelace, Nucl. Phys. B40 (1972) 157

26. The summary are seen in
C. Michael and R. Odorico, Phys. Letters 34B (1970) 422
C. Michael Springer Tracts in Modern Physics vol.55 (1970)

27. W. M. Smart, A. Kernan, G. E. Kalmus and R. P. Ely, Jr.
Phys. Rev. Letters 17 (1966) 556
P. J. Litchfield Nucl. Phys. B22 (1970) 269

28. C. Schmid and J. K. Storrow, Nucl. Phys. B29 (1971) 219

29. M. Imachi, T. Matsuoka, K. Ninomiya and S. Sawada
Prog. Theor. Phys. 40 (1968) 353
H. Harari Phys. Rev. Letters 22 (1969) 562
J. L. Rosner Phys. Rev. Letters 22 (1969) 689

30. M. Fukugita in preparation

31. C. Schmid Lett. Nuovo Cim. 1 (1969) 165

32. C. Bricman, E. Pagiola and C. Schmid, Nucl. Phys. B33 (1971) 135

33. V. Chabaud et al. Phys. Letters 38B (1972) 445

34. C. Schmid Proc. of Amsterdam Conference on Elementary Particles (1971)

35. M. Ademollo, H. R. Rubinstein, G. Veneziano and M. A. Virasoro Phys. Rev. 176 (1968) 1904

36. M. Davier and H. Harari, Phys. Letters 35B (1971) 239

37. J. D. Jackson Proc. of Lund Conference on Elementary Particles (1969)

This is a good summary of the trials in hadronic interactions till 1969.

Table 1

		momentum range (GeV/c)	method	highest partial waves
$\bar{K}N \to \bar{K}N$	Bricman et al. [11]	0.98 - 1.34	energy dep.	F_{15}, G_{07}
	Conforto et al. [12]	0.80 - 1.20	energy dep.	F_{15}, G_{07}
	Litchfield et al. [13]	1.26 - 1.84	energy dep.	G_{19}, G_{09}
$K^+p \to K^+p$	Albrow et al. [14] Sol.γ	0.14 - 2.50	energy indep.	$H_{1\,11}$
$KN \to KN$	Giacomelli et al. [15] Sol.III Wilson et al. [16] Sol.D	0.14 - 1.50	energy dep.	D_{15} D_{05}

Table 2

		t-ch.exchange	$\bar{f}_{++}$	$\bar{f}_{+-}/\sqrt{s}$	
$\bar{K}N \to \bar{K}N$	$I_t=0$	f + ω	$\Lambda_\alpha+\Lambda_\gamma+3(\Sigma_\delta+\Sigma_\beta)$	$-(\Lambda_\alpha+\Lambda_\gamma)+3(\Sigma_\delta+\Sigma_\beta)$	$\bar{f}_{++} >> \bar{f}_{+-}/\sqrt{s}$
	$I_t=1$	ρ + A_2	$\Lambda_\alpha+\Lambda_\gamma-(\Sigma_\delta+\Sigma_\beta)$	$-(\Lambda_\alpha+\Lambda_\gamma)-(\Sigma_\delta+\Sigma_\beta)$	$\bar{f}_{++} << \bar{f}_{+-}/\sqrt{s}$
$\pi N \to \pi N$	$I_t=0$	f	$N_\alpha+N_\gamma+2\Delta_\delta$	$-(N_\alpha+N_\gamma)+2\Delta_\delta$	$\bar{f}_{++} >> \bar{f}_{+-}/\sqrt{s}$
	$I_t=1$	ρ	$N_\alpha+N_\gamma-\Delta_\delta$	$-(N_\alpha+N_\gamma)-\Delta_\delta$	$\bar{f}_{++} << \bar{f}_{+-}/\sqrt{s}$
$\bar{K}N \to \pi\Lambda$	$I_t=1/2$	$K^* - K^{**}$	$\Sigma_\alpha-\Sigma_\gamma+\Sigma_\delta-\Sigma_\beta$	$-\Sigma_\alpha+\Sigma_\gamma+\Sigma_\delta-\Sigma_\beta$	

Figure captions

Fig.1 π^+p (a) and π^-p (b) polarizations at all angles from 1.60 to 2.31 GeV/c.[2] The solid and dashed curves represent the reconstructions from the previous partial wave analyses of CERN (exper.) and Berkeley respectively. The dotted curve (a) and dash-dotted curve (b) represent the low energy extrapolations of the FESR Regge pole fit[3] with P, P', P", ρ and ρ'. [Figure from ref.2]

Fig.2 Comparison of the imaginary part of $K^-p \to \bar{K}^0n$ scattering amplitude (dashed curves) with those of the resonance contribution (solid curve) in the forward direction. We take the amplitude $\bar{f}_{+-} = f_{+-}/\sin\frac{\theta}{2}$ calculated from the partial wave solutions.[11-13] [ref.9]

Fig.3 t-dependence of the imaginary parts of the s-channel helicity amplitudes constructed from the background parts of the $\bar{K}N$ partial wave amplitudes of ref.11 (a) (b) and ref.13 (a') (b'). The figures on the curves represent the values of the incident momentum p_{Lab} in GeV/c units. [ref.9]

Fig.4 t-dependence of the imaginary parts of the s-channel helicity amplitudes at 1.5 GeV/c constructed from the KN partial wave amplitudes of ref.15 and 16. [ref.17]

Fig.5 Energy dependence of the imaginary parts of the $I_t=0$ $\bar{K}N$ forward background amplitude (solid curve) as compared with that of the $I_t=0$ forward amplitude calculated from K^+p and K^+n total cross section data. Also shown is the extrapolation (linear in s) of the high energy amplitude corresponding to $\sigma_{KN}(\infty) = 18$ mb. [ref.9]

Fig.6 t-dependence of the imaginary parts of the s-channel helicity amplitudes (solid curve) at p_{Lab} = 1.0 (I), 1.1 (II), 1.2 (III) and 1.3 (IV) (GeV/c) constructed from the resonant parts of ref.11. Total amplitude (= resonant part + background part, dashed curve) at p_{Lab} = 1.0 GeV/c are also shown for comparison. [ref.9]

Fig.7 Partial wave profiles of the imaginary parts of the resonant parts of the $\bar{K}N$ helicity amplitudes at p_{Lab} = 0.8 $\sim$ 1.8 GeV/c. Where the impact parameter b is defined as $J = b \cdot q$ (q ; c.m. momentum). [ref.21]

Fig.8 t-dependence of the real part of the s-channel helicity flip amplitude of $K^- p \to \bar{K}^0 n$ (I_t=1) at several values of p_{Lab}. The partial wave solutions of refs.[11, 13] are used. [ref.9]

Fig.9 t-dependence of the real part of the s-channel helicity flip amplitude corresponding to $f(K^- p) - f(K^+ p)$. at several values of p_{Lab}. The partial wave solutions of ref.[13, 14] are used. [ref.17]

Fig.10 Partial wave profiles of the imaginary part of the helicity flip amplitude of $\pi^- p \to \pi^0 n$ at p_{Lab} = 1.2 and 1.6 (solid curve) calculated from the CERN partial wave solution[25]. The dashed curve represents the partial wave projection of phenomenological Regge fit[3] at each energy. [ref.21]

Fig.11 Partial wave profiles of the imaginary parts of the helicity amplitudes of $K^-p \to \pi\Lambda$ at p_{Lab} = 1.0 - 1.8 GeV/c calculated from the partial wave solution of ref.27 (Litchfield). (b = J/q)

Fig.12 πNN coupling strength calculated by the extrapolation of the I_u = 1/2 πN scattering amplitude to the nucleon pole $u = M_N^2$. [ref.30]

Fig.13 The imaginary and real parts of the backward scattering amplitude of $K^-p \to \bar{K}^0n$. The solid curves are computed from the partial wave analyses and the dashed curves are contribution coming from resonances only. [ref.32]

Fig.14 The impact parameter profile of the imaginary part of the helicity nonflip amplitude calculated as

$$Imf_{++} \simeq \frac{\frac{d\sigma}{dt}(K^-p) - \frac{d\sigma}{dt}(K^+p)}{2\sqrt{\frac{d\sigma}{dt}(K^+p)}}$$

at 5 GeV/c. [ref.36]

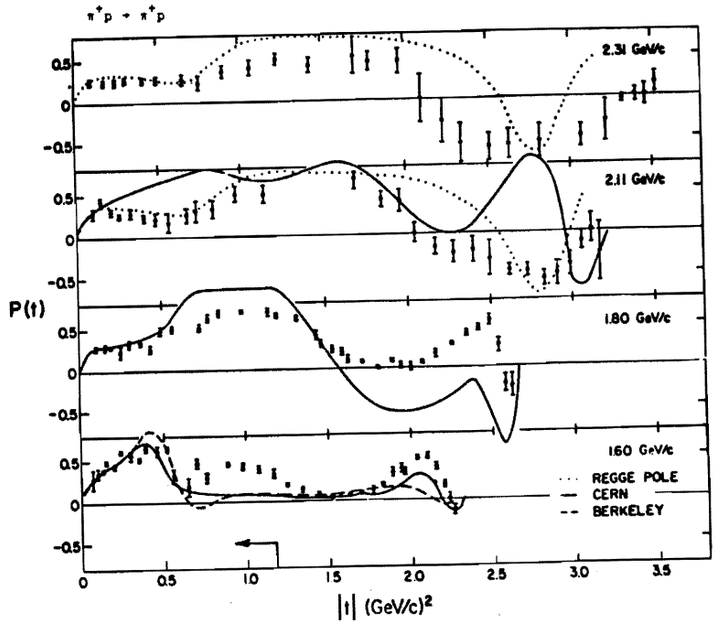
$\pi^+p \to \pi^+p$
2.31 GeV/c
2.11 GeV/c
1.80 GeV/c
1.60 GeV/c
REGGE POLE
CERN
BERKELEY
P(t)
|t| (GeV/c)²

Fig.1 (a)

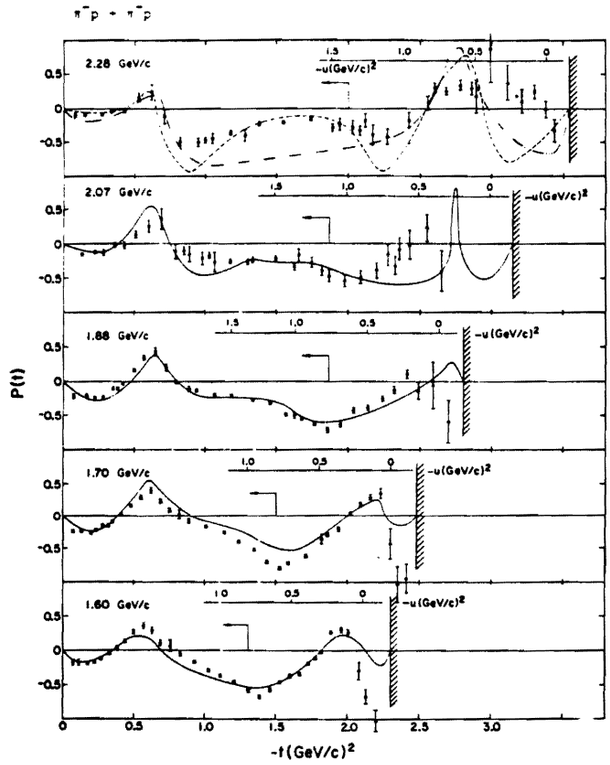
$\pi^-p \to \pi^-p$
2.28 GeV/c
2.07 GeV/c
1.88 GeV/c
1.70 GeV/c
1.60 GeV/c
-u(GeV/c)²
P(t)
-t(GeV/c)²

Fig.1 (b)

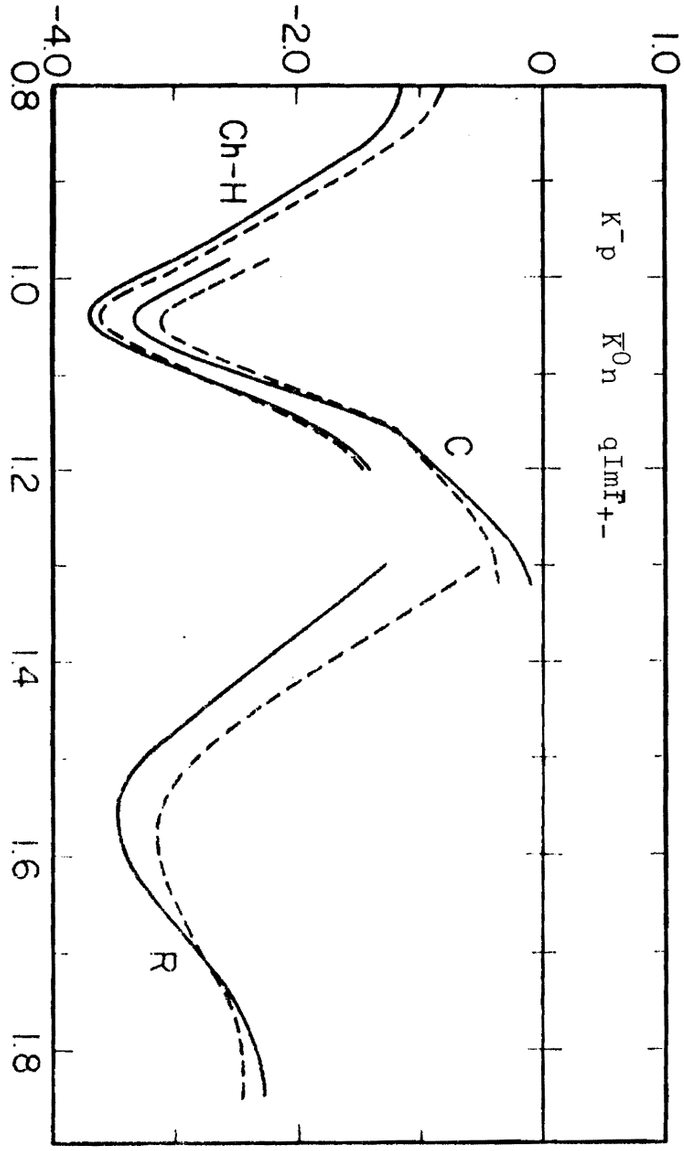

Fig.2

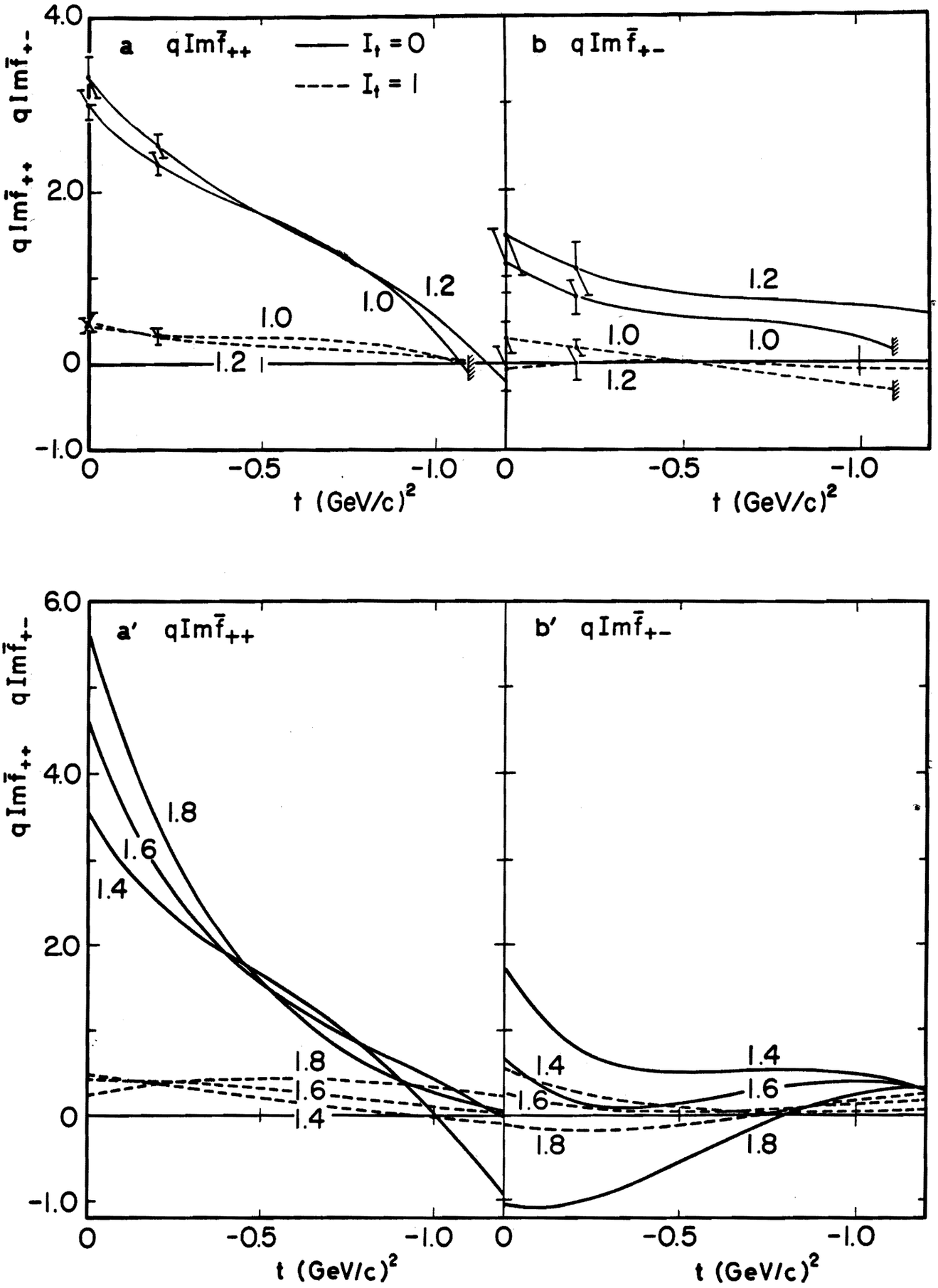
a qImf̄++
I_t = 0
I_t = 1
b qImf̄+-
qImf̄++ qImf̄+-
4.0
2.0
0
-1.0
1.2
1.0
1.0
1.2
1.2
1.0
1.0
1.2
0
-0.5
-1.0
t (GeV/c)²
a' qImf̄++
b' qImf̄+-
6.0
4.0
2.0
0
-1.0
1.8
1.6
1.4
1.8
1.6
1.4
1.4
1.6
1.8
1.4
1.6
1.8

Fig.3

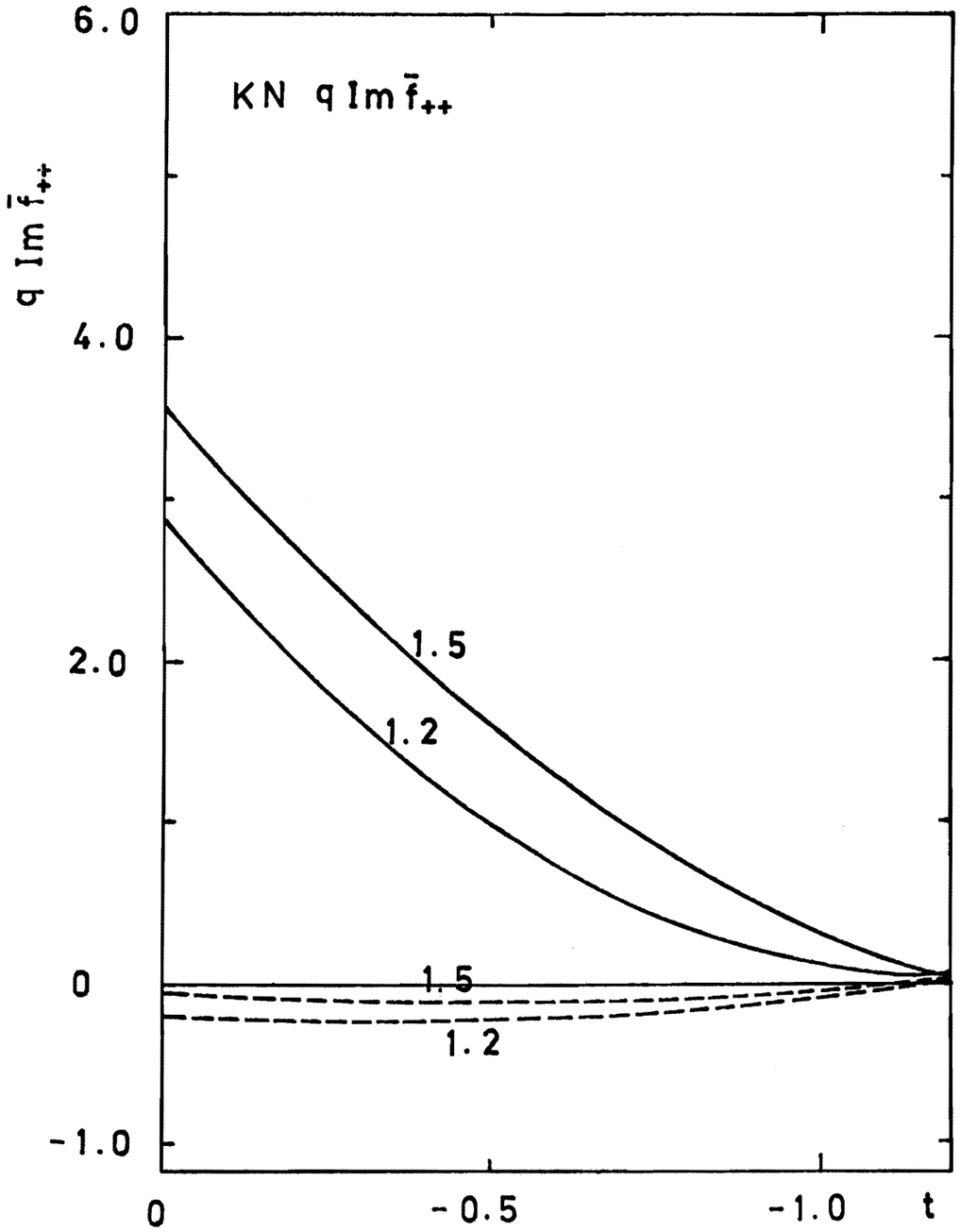

Fig.4

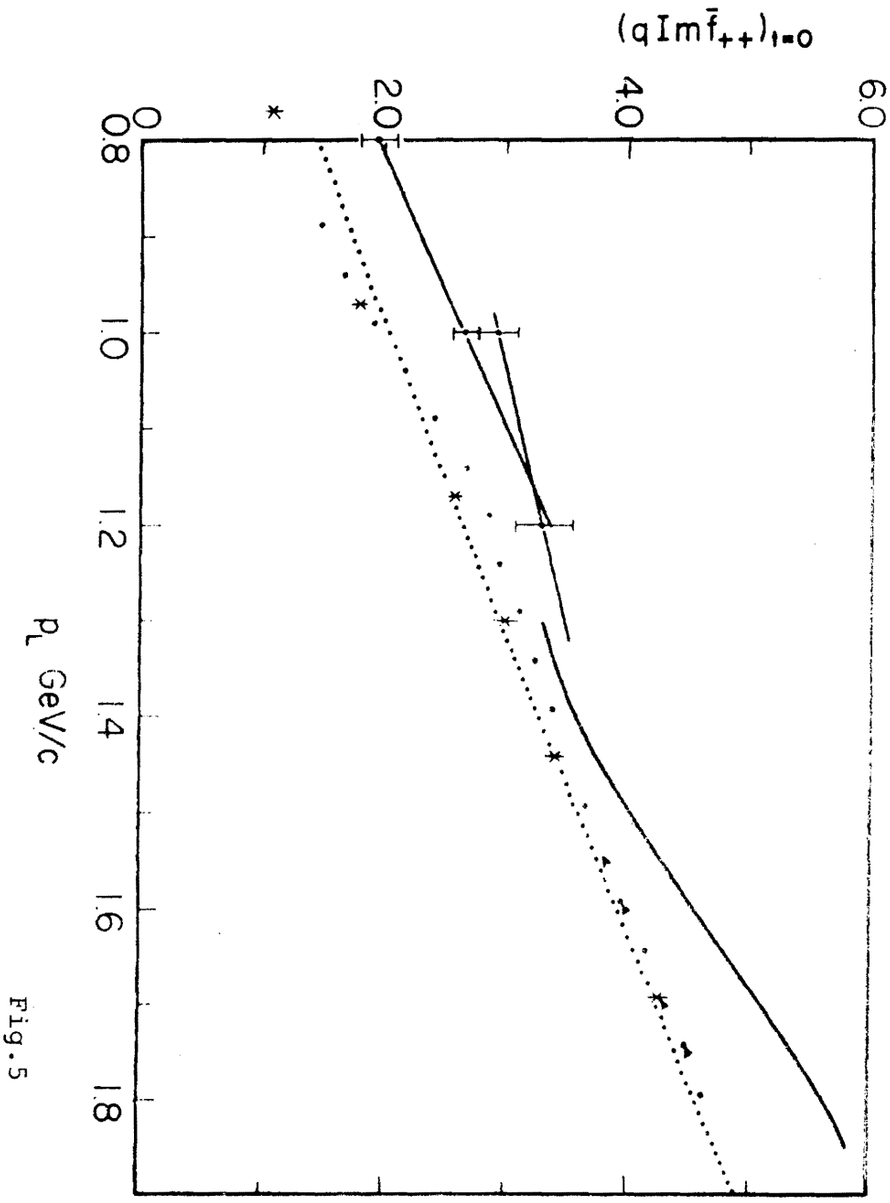

Fig.5

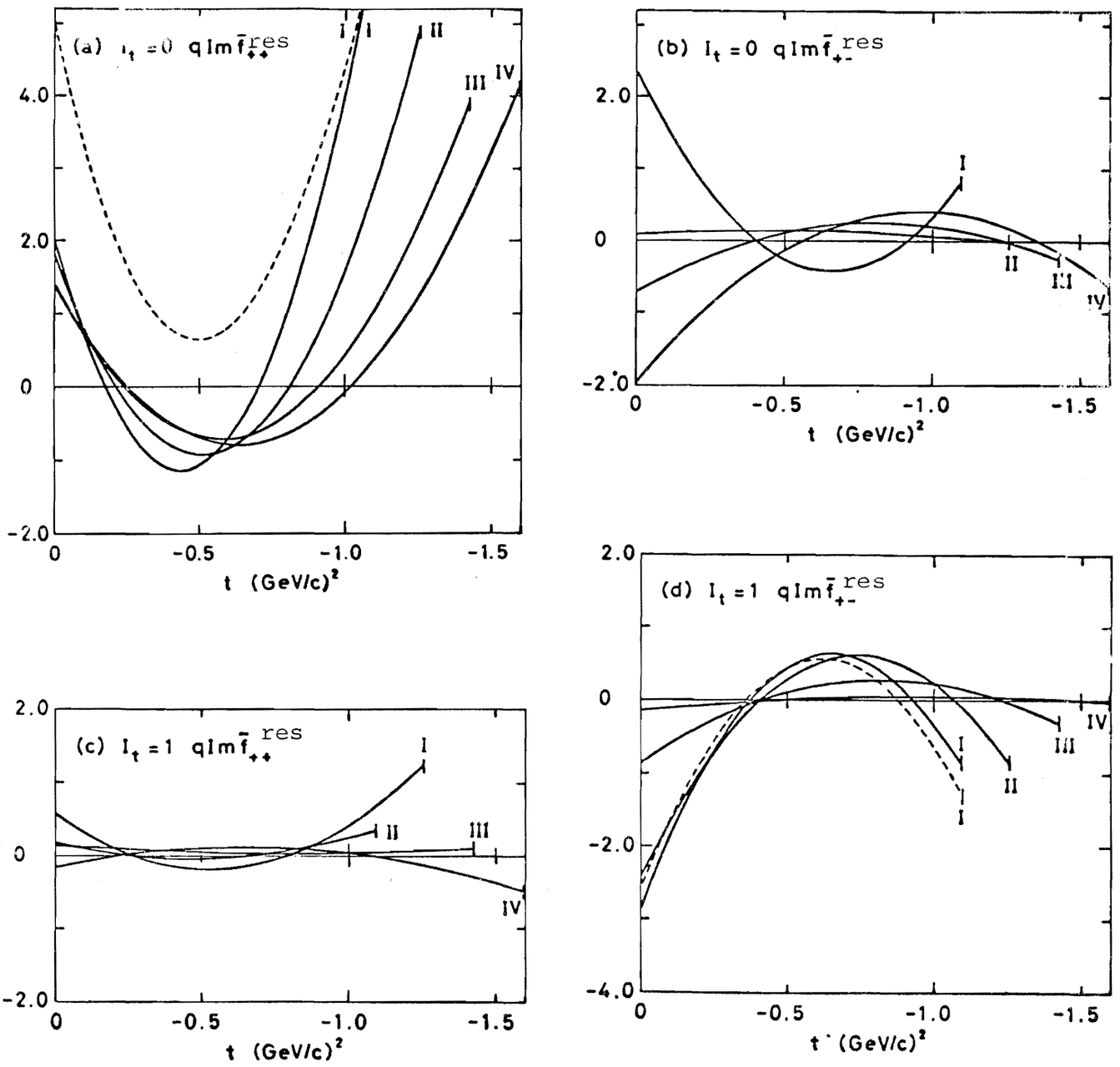
(a) $I_t=0$ $q\,\mathrm{Im}\bar{f}^{res}_{++}$
(b) $I_t=0$ $q\,\mathrm{Im}\bar{f}^{res}_{+-}$
(c) $I_t=1$ $q\,\mathrm{Im}\bar{f}^{res}_{++}$
(d) $I_t=1$ $q\,\mathrm{Im}\bar{f}^{res}_{+-}$
I
II
III
IV
t (GeV/c)²

Fig. 6

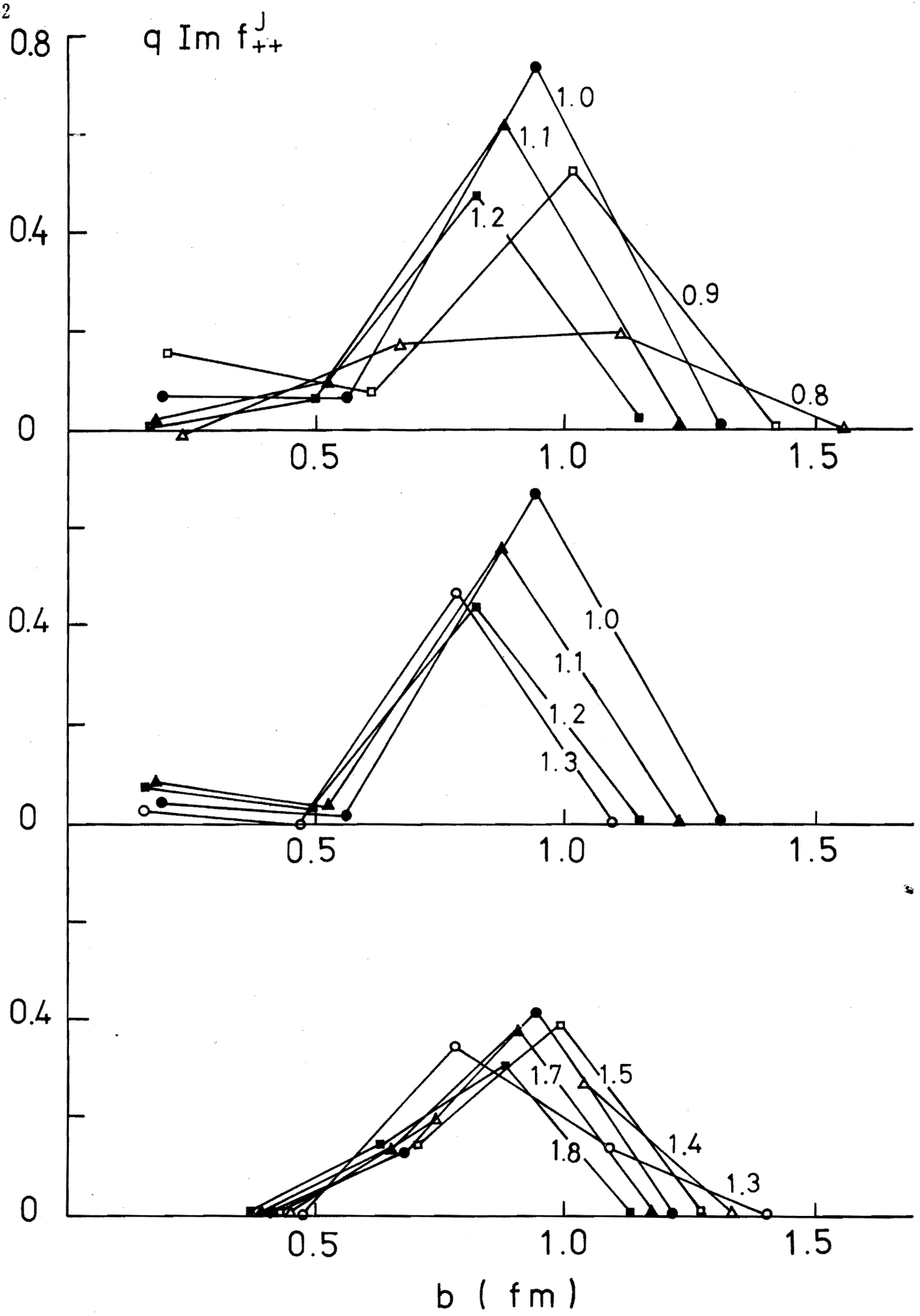
q Im f^J_{++}
0.8
0.4
0
1.0
1.1
1.2
0.9
0.8
0.5
1.0
1.5
0.4
0
1.0
1.1
1.2
1.3
0.5
1.0
1.5
0.4
0
1.7
1.5
1.8
1.4
1.3
0.5
1.0
1.5
b (fm)

Fig.7 (a)

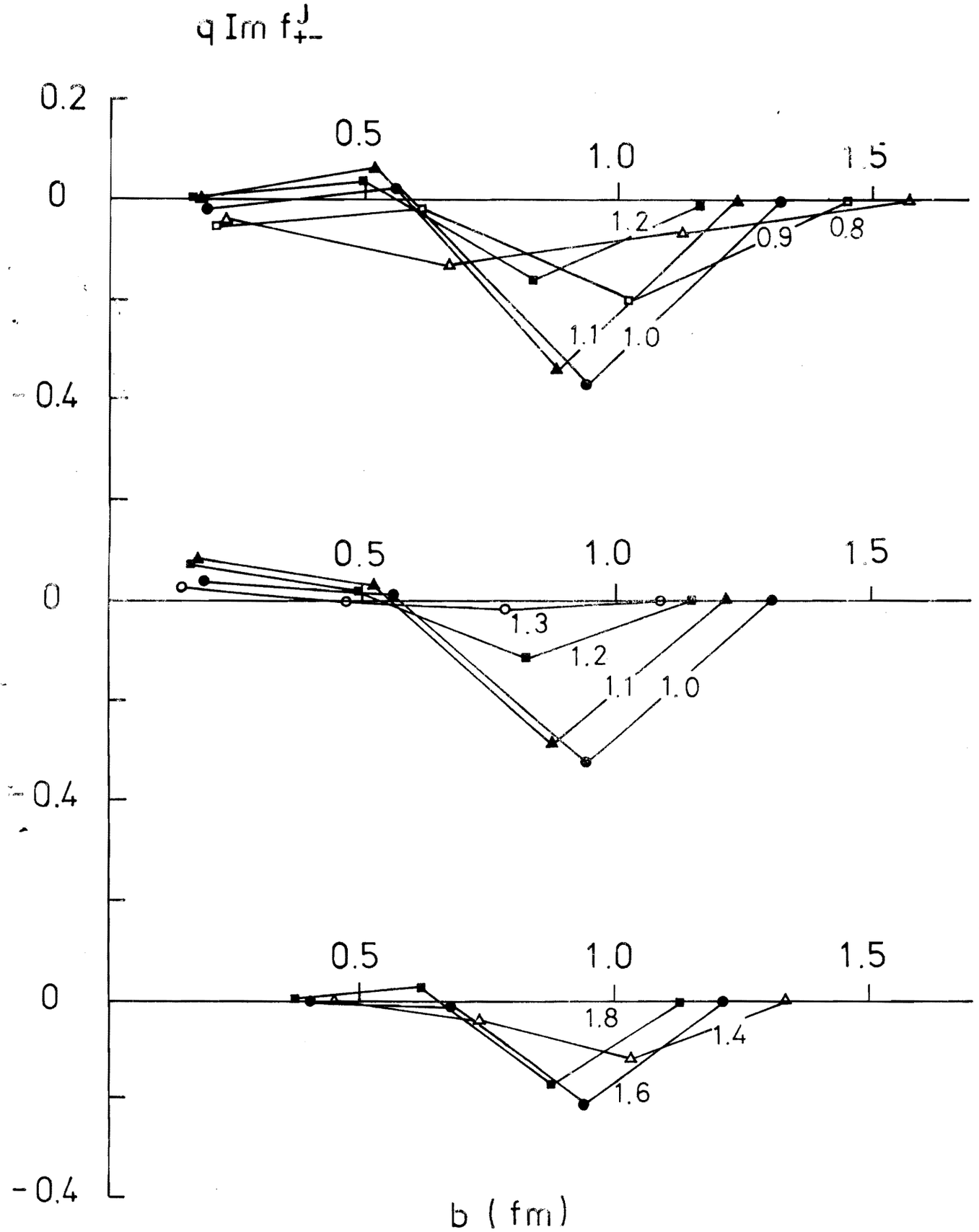

Fig.7 (b)

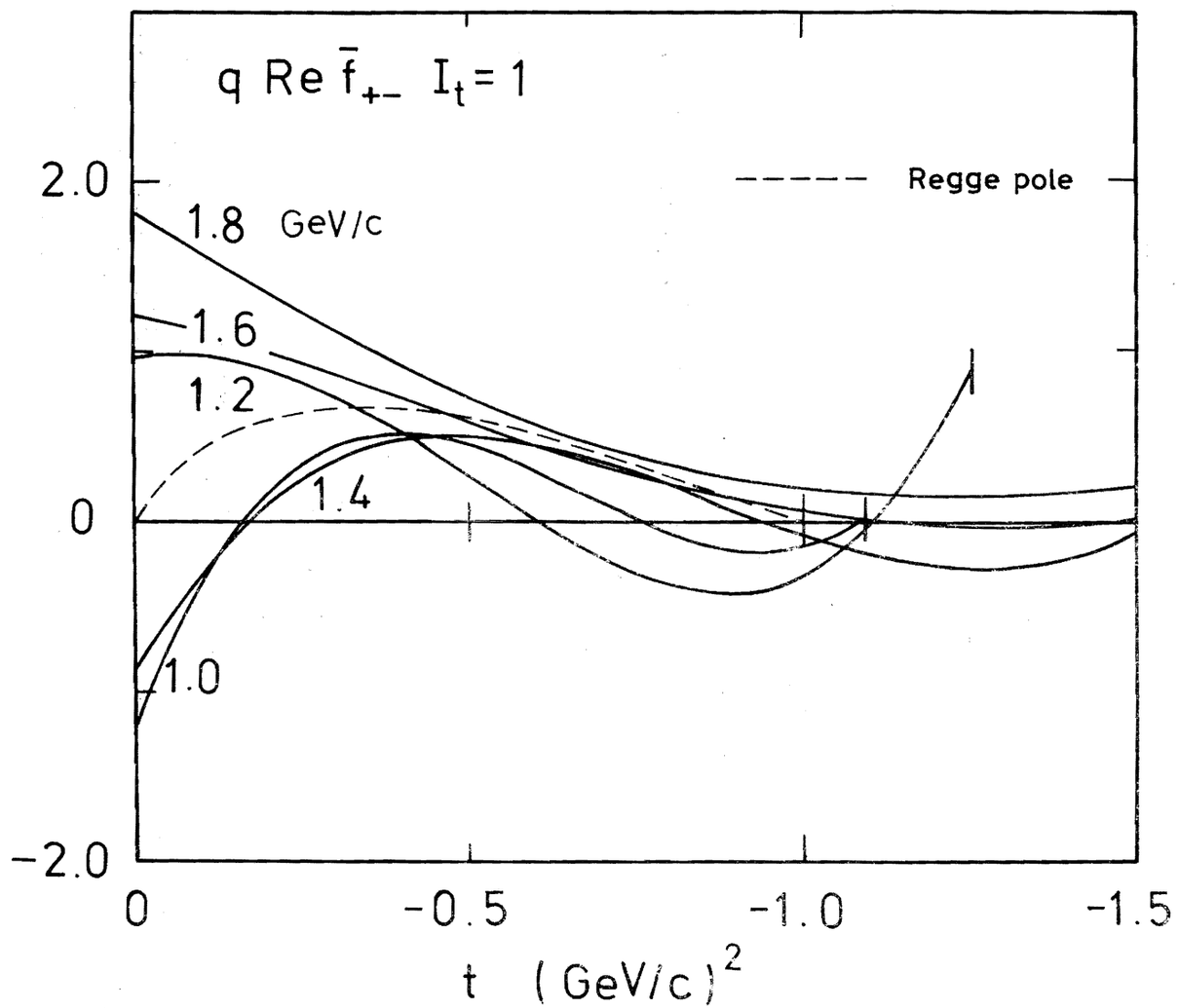
q Re $\bar{f}_{+-}$ $I_t = 1$
Regge pole
1.8 GeV/c
1.6
1.2
1.4
1.0
2.0
0
-2.0
0
-0.5
-1.0
-1.5
t (GeV/c)^2

Fig.8

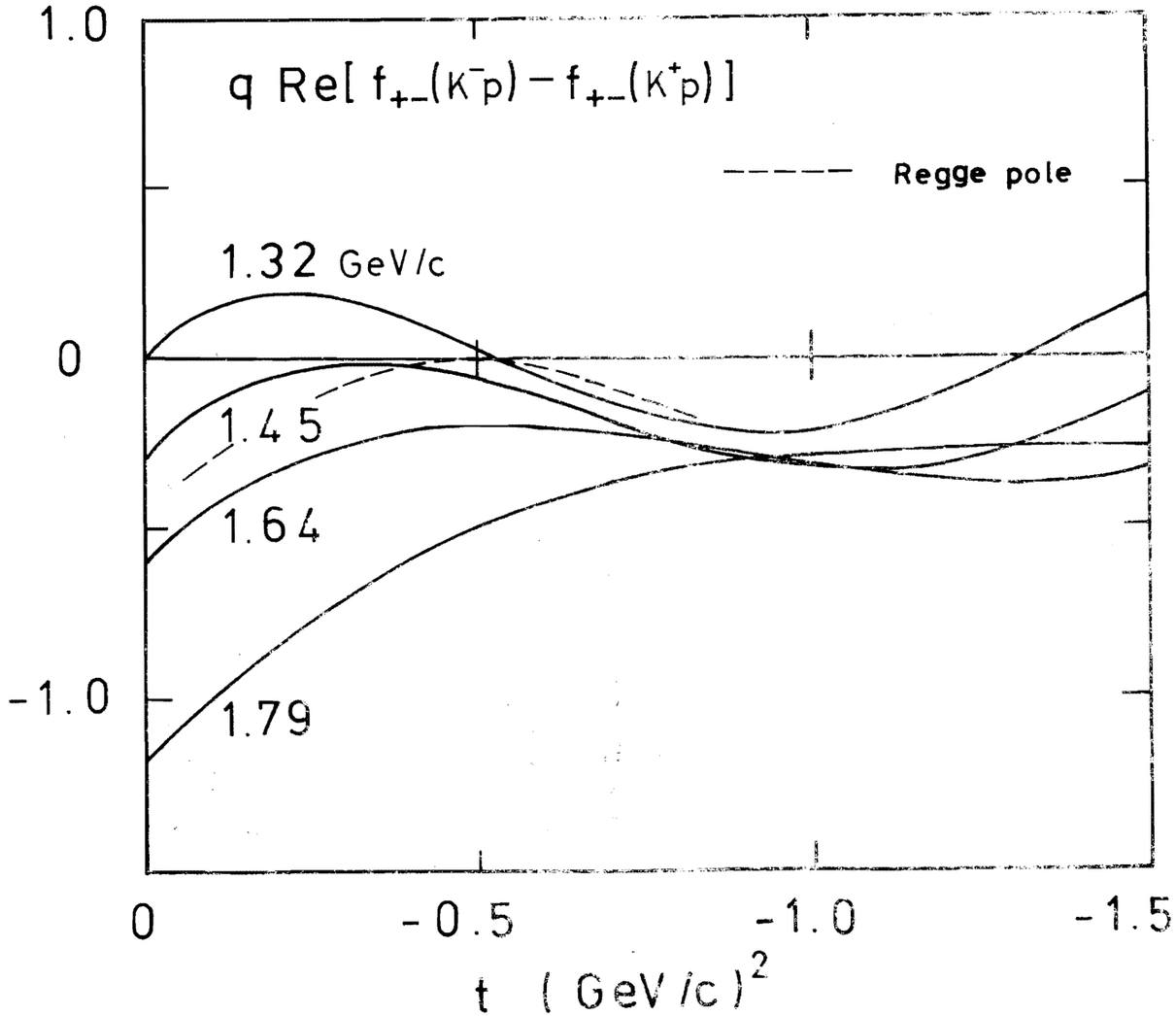
1.0
q Re[f+-(K⁻p) − f+-(K⁺p)]
Regge pole
1.32 GeV/c
0
1.45
1.64
-1.0
1.79
0
-0.5
-1.0
-1.5
t (GeV/c)²

Fig.9

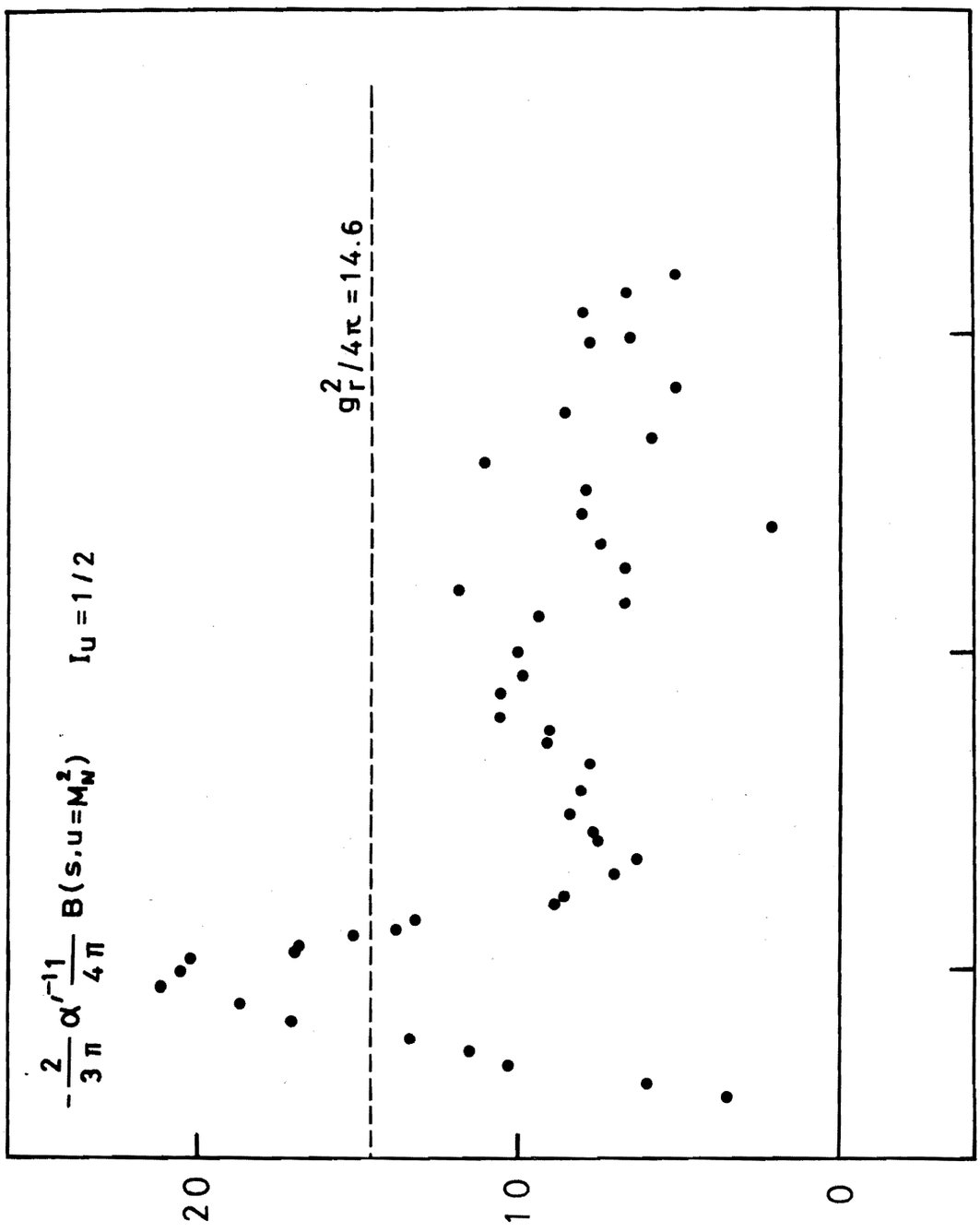
$-\frac{2}{3\pi}\alpha'^{-1}\frac{1}{4\pi}B(s,u=M_N^2)$
$I_u = 1/2$
$g_r^2/4\pi = 14.6$
20
10
0
1.0
1.5
2.0
P_L
(GeV/c)

Fig.12

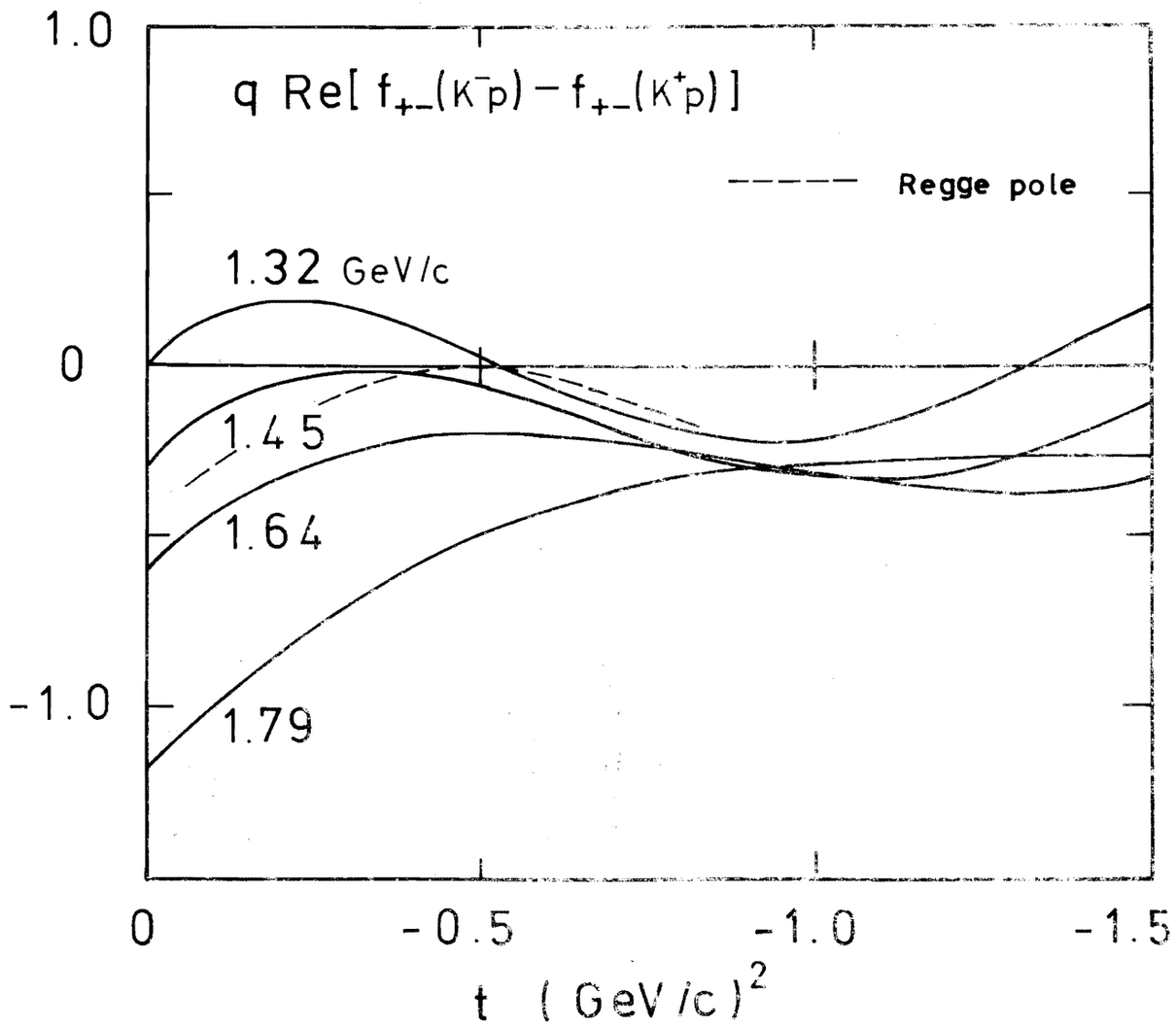
1.0
q Re[f+-(K⁻p) − f+-(K⁺p)]
Regge pole
1.32 GeV/c
0
1.45
1.64
-1.0
1.79
0
-0.5
-1.0
-1.5
t (GeV/c)²

Fig.9

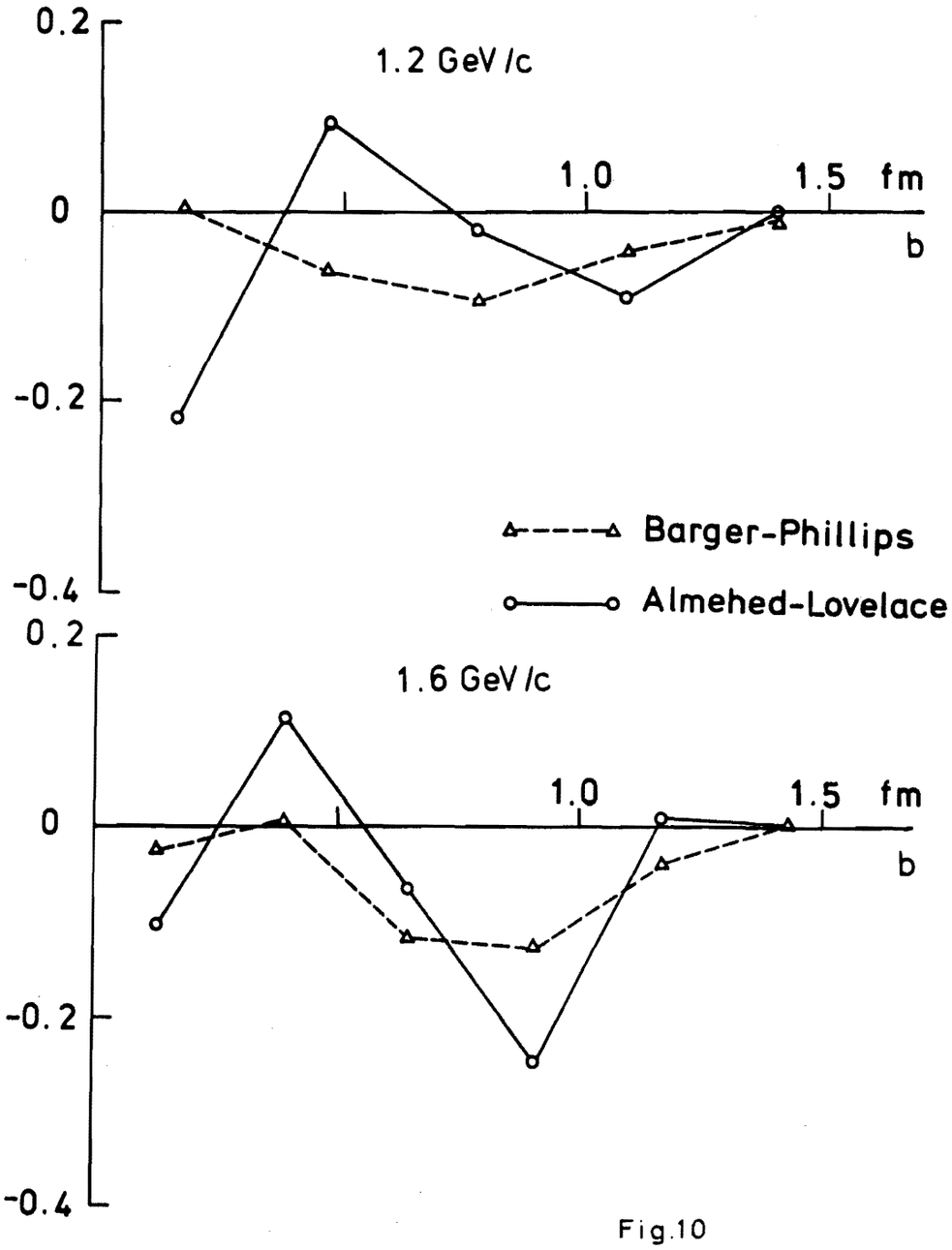
0.2
1.2 GeV/c
1.0
1.5 fm
0
b
-0.2
-0.4
Barger-Phillips
Almehed-Lovelace
0.2
1.6 GeV/c
1.0
1.5 fm
0
b
-0.2
-0.4

Fig.10

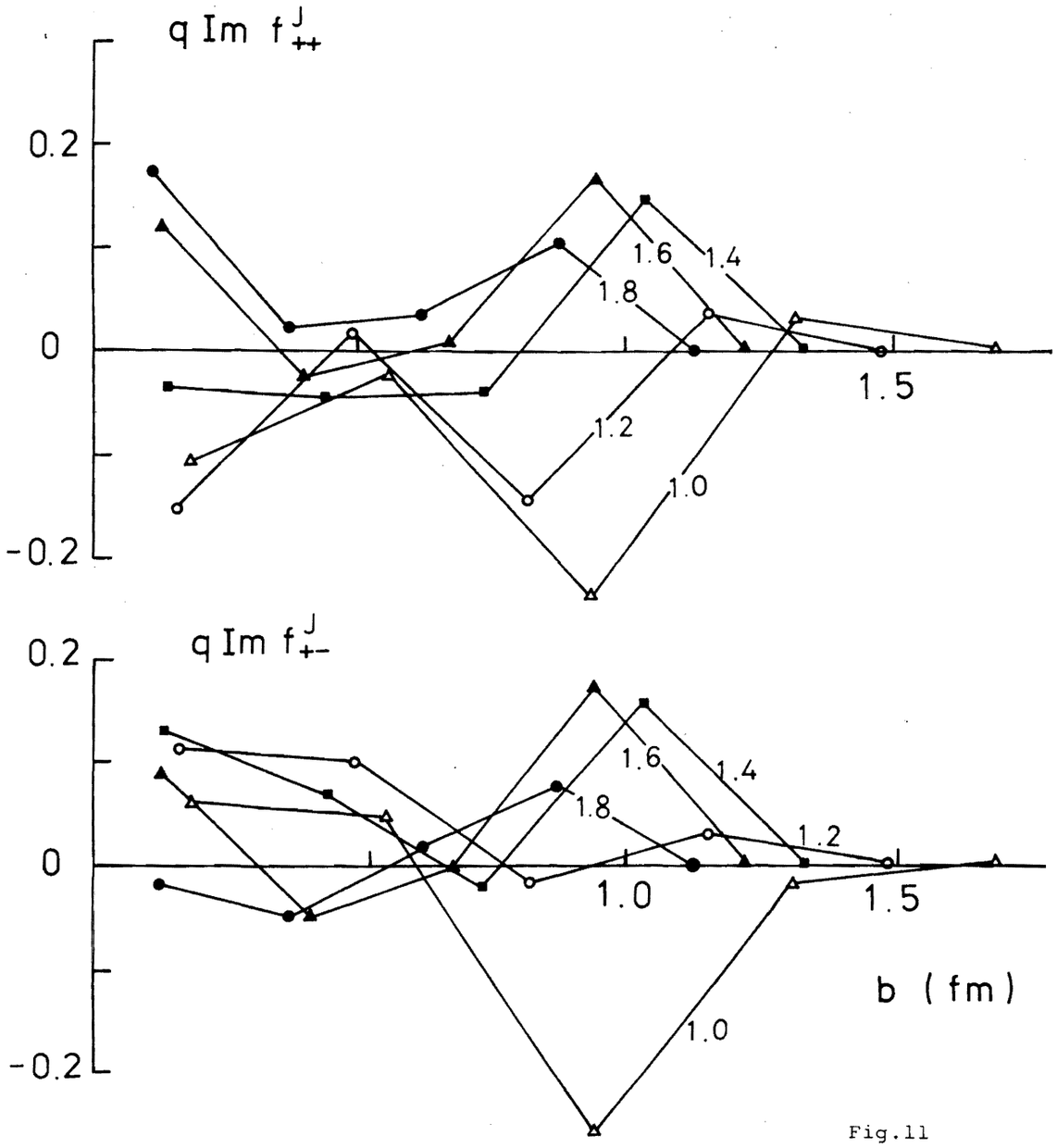

Fig.11

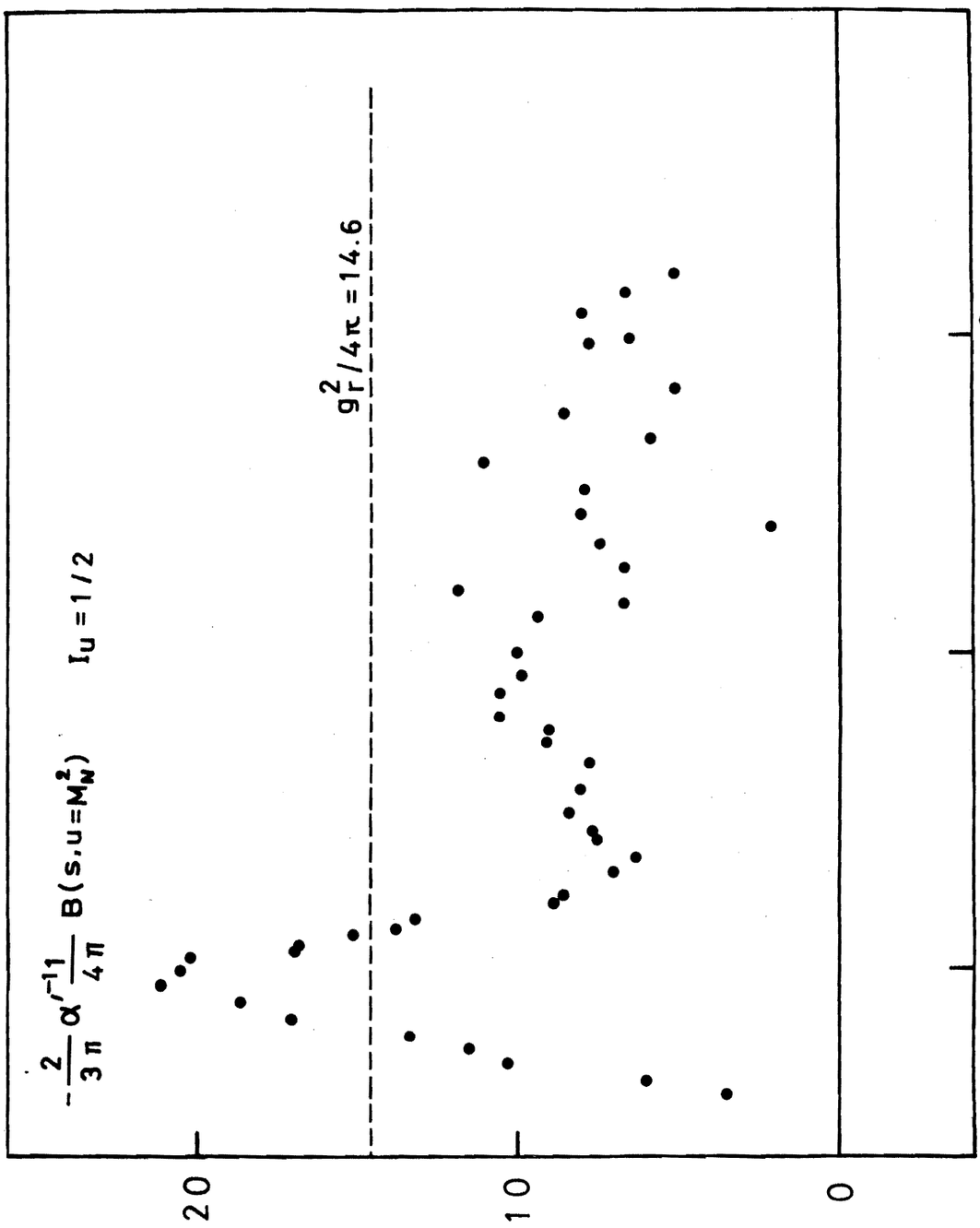
$-\frac{2}{3\pi}\alpha'^{-1}\frac{11}{4\pi}B(s,u=M_N^2)$
$I_u=1/2$
$g_r^2/4\pi=14.6$
20
10
0
1.0
1.5
2.0
P_L
(GeV/c)

Fig.12

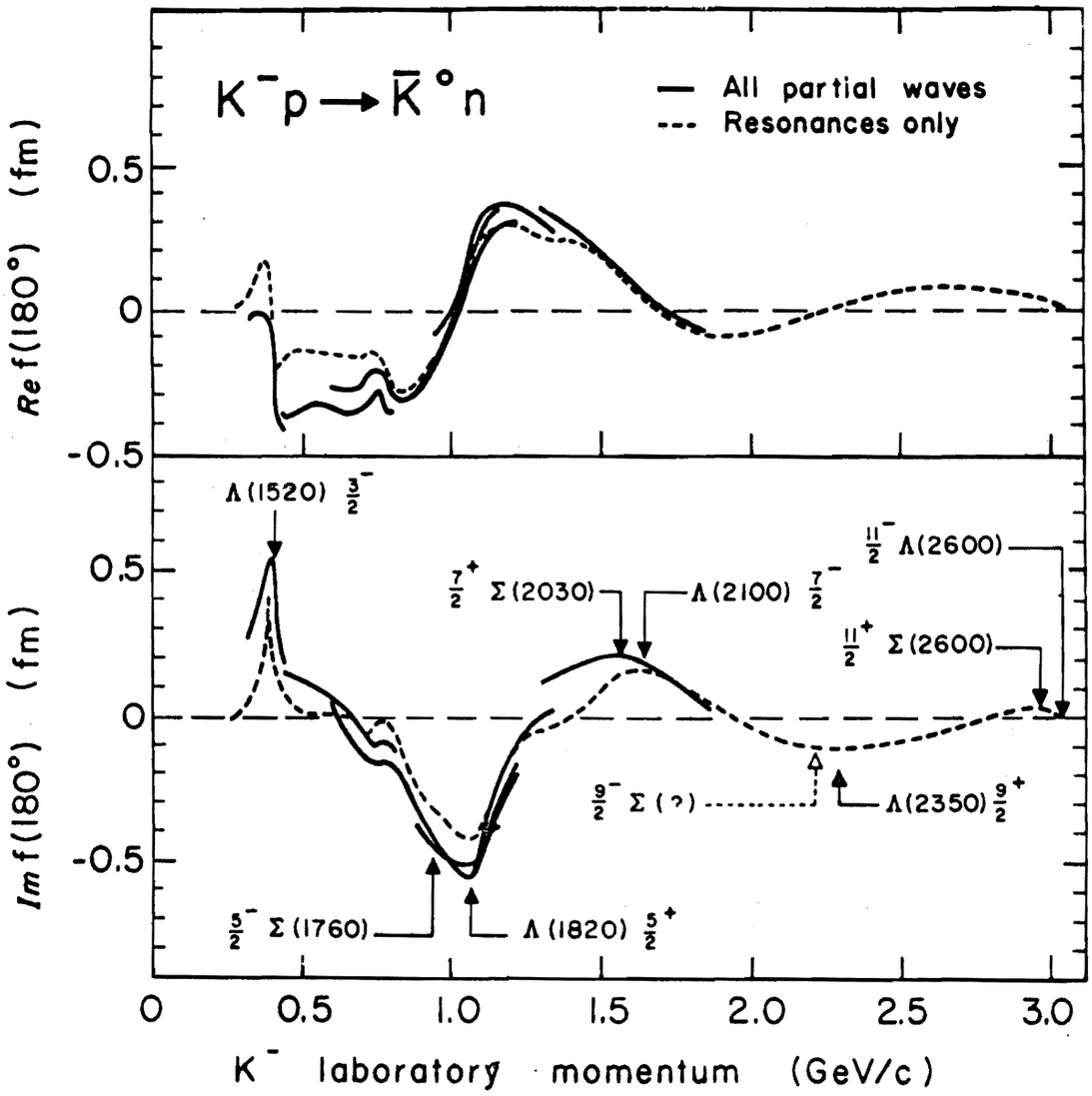
K⁻p → K̄°n
All partial waves
Resonances only
Re f(180°) (fm)
Im f(180°) (fm)
0.5
0
-0.5
Λ(1520) 3/2⁻
7/2⁺ Σ(2030)
Λ(2100) 7/2⁻
11/2⁻ Λ(2600)
11/2⁺ Σ(2600)
9/2⁻ Σ(?)
Λ(2350) 9/2⁺
5/2⁻ Σ(1760)
Λ(1820) 5/2⁺
0
0.5
1.0
1.5
2.0
2.5
3.0
K⁻ laboratory momentum (GeV/c)

Fig. 13

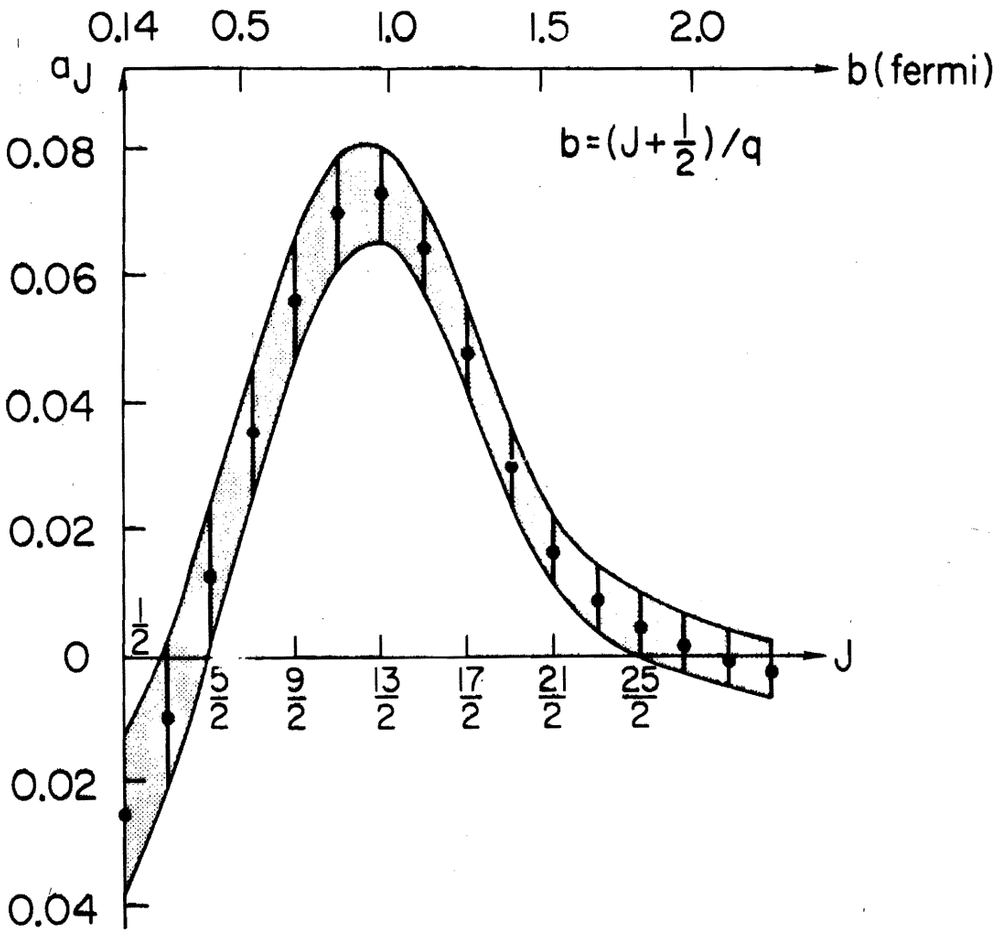
0.14
0.5
1.0
1.5
2.0
a_J
b (fermi)
$b=(J+\frac{1}{2})/q$
0.08
0.06
0.04
0.02
0
0.02
0.04
$\frac{1}{2}$
$\frac{5}{2}$
$\frac{9}{2}$
$\frac{13}{2}$
$\frac{17}{2}$
$\frac{21}{2}$
$\frac{25}{2}$
J

Fig.14

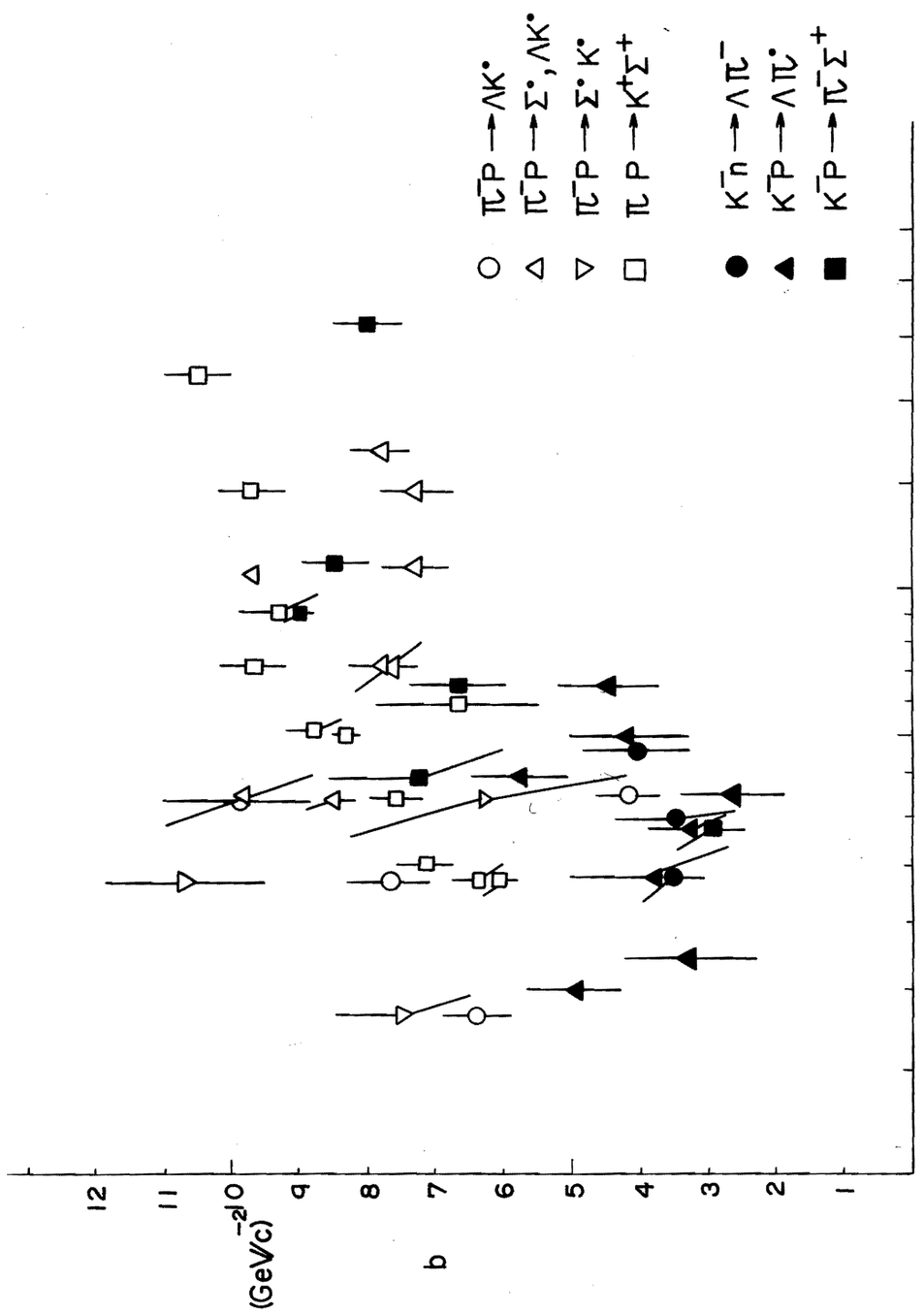
$\pi^- P \to \Lambda K^\circ$
$\pi^- P \to \Sigma^\circ, \Lambda K^\circ$
$\pi^- P \to \Sigma^\circ K^\circ$
$\pi^- P \to K^+ \Sigma^+$
$K^- n \to \Lambda \pi^-$
$K^- P \to \Lambda \pi^\circ$
$K^- P \to \pi^- \Sigma^+$
b
$(GeV/c)^{-2}$
S $(GeV)^2$

Fig. 3 (a)

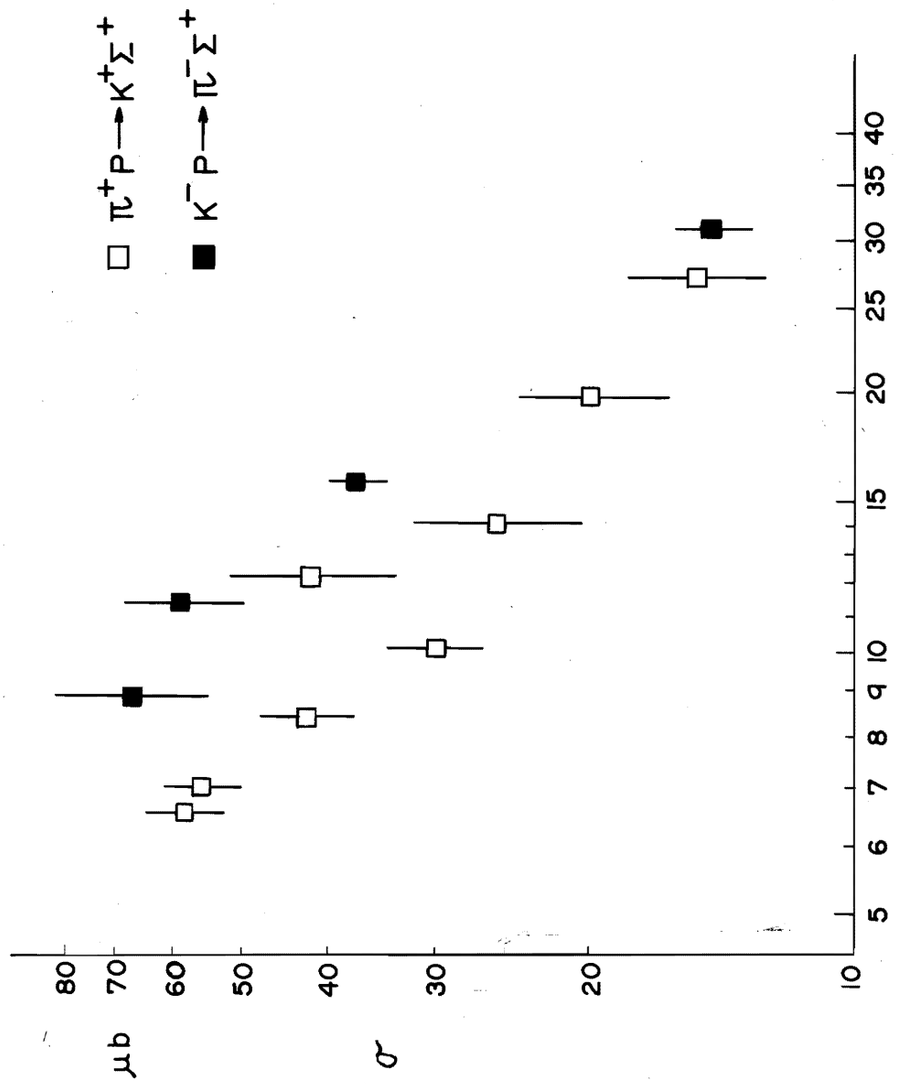

Fig. 3 (b)